Iraqi Journal for Applied Science (IJAS)
Vol. 3, No. 1, March 2026, pp. 54-66
ISSN: 3006-5828, DOI: 10.69923/25avbz81

Synthesis, characterization, and biological evaluation of some Mercury (II) complexes with mixed 3-hydroxy-N'-(2-oxoindolin-3-ylidene)-2-naphthohydrazide and phosphine ligands

Ali Hussien Ali, Ahmed A. Irzoqi, Yuosra K. Alasadi
Department of Chemistry, College of Education for Pure Science, University of Tikrit, Tikrit, Iraq

Article Info

Article history:

Received: 04, 10, 2025
Revised: 30, 11, 2025
Accepted: 30, 01, 2026
Published: 30, 03, 2026

Keywords:

mercury complexes,
Isatin,
Phosphines,
biological evaluation.

ABSTRACT

Several mercury (II) complexes were prepared with the ligand (L), (E)-3-hydroxy-N'-(2-oxoindolin-3-ylidene)-2-naphthohydrazide, and mixed ligands like (dppm) bis(diphenylphosphino) methane, and (dppp) bis(diphenylphosphino)propane. They were characterized using elemental analysis, molar conductivity, FTIR, ^{1}H, ^{13}C, ^{31}P NMR, EDS, Mass, and TGA. The analyses indicate that Hg(II) complexes are square planar, with the ligand (L) coordinating through oxygen and nitrogen. The proposed formulas are $[Hg2(L2)_2(\mu\text{-dppm})_2]Cl_4$ and $[Hg(L2)(dppp)]Cl_2$. These ligands coordinate differently: (dppm) as bridging in binuclear complexes, and (dppp) as bidentate in dinuclear complexes. XRD analysis revealed complexes with crystallinity ranging from 23.49% to 28.06% and sizes varying from 8.27280648 to 183.4763452nm. The compounds showed good activity against Staphylococcus aureus and Pseudomonas aeruginosa, except for the ligand.

Corresponding Author:

Ali Hussein Ali Nima Al-Khazraji
College of Education for Pure Sciences, Tikrit University, Iraq.
Email: ah244006pep@st.tu.edu.iq

1. INTRODUCTION

Preparation of Schiff base derivatives plays a crucial role in various scientific disciplines. Recent data from the Scopus database indicate that nearly 2,000 papers are published annually in this field[1]. Schiff base derivatives are an essential class of organic compounds due to their ability to form complexes with transition-metal ions via the nitrogen atom of the azomethine group, making them a heavily researched area [2]. The resulting complexes have a broad spectrum of applications, including analytical, biological, industrial, and clinical sectors, as well as essential roles in organic synthesis and catalysis [3]. Isatins are compounds with considerable structural versatility, as they can be used to produce various heterocyclic compounds, including quinolones and indole derivatives, making them valuable precursors in drug synthesis. Isatin has also been detected in mammalian tissues, sparking interest in studying it as a modulator in several biochemical processes[4]. Isatin derivatives have significant applications, exhibiting biological properties such as anticonvulsant[5], antidepressant[6], anti-inflammatory[7], anticancer[8], antifungal[9], and anti-HIV activities[10]. Isatin and its derivatives are captivating and versatile building blocks that are extensively utilized in the synthesis of significant and bioactive heterocyclic compounds[11], [12], [13], [14]. Hydrazine's and hydrazones are of significant importance in chemical and biological settings due to their flexible structures and reactivity. They have also been utilized as synthetic intermediates to produce numerous molecular hybrids, with applications ranging from potential pharmaceuticals to industrial agents[15], [16]. Metal complexes have attracted significant attention due to their diverse applications in biology, medicine, and environmental remediation [17], [18], [19]. Both thiosemicarbazones and isatin are among the most essential ligands, as they can form stable and biologically active metal complexes[20], [21]. Combining with metal ions enhances the biological activity of isatin ligands. The study of interactions between different metal ions and ligands, particularly mixed-ligand complexes, is an active area of research, as these complexes often show greater effectiveness compared to their individual ligands[22], [23].

Recently, tertiary phosphines (PR_3) and related molecules have been recognized as one of the most important families of ligands, having a significant impact on organometallic chemistry and homogeneous catalysis[23], [24], [25]. This is due to their strong influence on the stability and reactivity of transition metal complexes. These ligands are characterized by the ease with which their electronic and steric properties can be tuned through variation of the substituents attached to the phosphorus atom, making them highly effective tools for designing complexes tailored to specific applications. Their importance lies in their central role in homogeneous catalysis, where they have made significant contributions to the development of numerous industrial and laboratory catalytic reactions, including carbon–carbon (C–C) and carbon–nitrogen (C–N) bond-forming reactions. Furthermore, the ability of phosphines to vary their steric profile and electron-donating strength provides great flexibility to adapt to the requirements of different metal ions, making them among the most widely used ligands in pharmaceutical, petrochemical, and industrial catalysis[26], [27], [28].

Researchers have long been fascinated by metal complexes due to their vital role in various fields, particularly those that benefit society, such as medicine and industry. Interest in these compounds surged following the discovery of the first effective anticancer drug, cisplatin (cis-diamminedichloropalladium(II))[29]. Further discoveries and notable innovations soon followed this breakthrough in preparing such complexes, which have had a profound impact on humanity's ability to combat all types of malignant tumors.

2. Experimental Part

Raw chemicals and solvents were used without purification, and Sigma-Aldrich and Fluka supplied all materials. Melting points of the complexes were determined using a Stuart Melting Point apparatus. The infrared spectra were recorded on an FTIR-8400s instrument from SHIMADZU, spanning 400-4000 cm^{-1}, with samples prepared as KBr tablets. ^{1}H-NMR, ^{13}C-NMR, and ^{31}P-NMR spectra were obtained using a Bruker instrument operating at 400 MHz, with (DMSO-d6) as the solvent.

2-1 Methods

Preparation of 3-hydroxy-N'-(2-oxoindolin-3-ylidene)-2-naphthohydrazide Ligand (L)

The ligand was prepared in two steps:

2-1-1 Preparation of 3-hydroxy-2-naphthohydrazide: Hydrazine (0.126 g, 10 mmol) was added directly to methyl 3-hydroxy-2-naphthoate (0.51g, 10 mmol). The mixture was then refluxed for three hours. Following reflux, the mixture was filtered, and the resulting solution was allowed to cool, yielding a precipitate. This precipitate was then filtered, rinsed with cold water, and dried. The final weight of the precipitate was 0.38 g, corresponding to a yield of 72.79%.

2-1-2 Preparation of a Schiff's Base from Isatin (L): A solution of 3-hydroxy-2-naphthohydrazide (0.647g, 10 mmol) in 10 mL of absolute ethanol was mixed with a suspension of isatin (0.471 g, 10 mmol) in 10 mL of absolute ethanol to which a few drops of glacial acetic acid were added. The resulting mixture was then refluxed for 3 hours. After reflux, the mixture was filtered and then washed with cold ethanol. The final weight of the precipitate was 0.987g, corresponding to a yield of 93.20%. The obtained product was then dried in a vacuum oven[30], [31].

(L) dark-yellow solid. Yield :(0.265gm, 92.49%). melting point 251-253 °C. IR (KBr, cm^{-1}): 3411.84m (OH), 1697.17s (C=O), 1664.45s(C=O), 1625.02m(C=N), 3247.90m (N-H), 3058.89m aromatic (C-H). ^{1}H-NMR (δppm, J Hz, DMSO-d^6), **δ** =14.54 (s, 1H, OH), **δ**= 11.78 (s, 1H, NH_{amid}), **δ**= 11.20 (s, 1H, NH_{isatin}), 8.70 (s, 1H, H_e), 8.02 (d, $^{3}J_{H-H}$ =8.24 Hz , 1H, H_f), **δ** =7.77 (d, $^{3}J_{H-H}$ = 8.36 Hz, H_i), **δ** =7.63 (d, $^{3}J_{H-H}$= 7.59 Hz, 1H, H_a), **δ** =7.53 (t, $^{3}J_{H-H}$=7.59Hz, 1H, H_c), **δ** =7.38 (m, 3H, H_j, H_g and H_h), **δ** =7.11 (t, $^{3}J_{H-H}$ = 7.47Hz, 1H, H_b), **δ** = 6.94 (d, $^{3}J_{H-H}$ = 7.76Hz, 1H, H_d), ^{13}C-NMR (δppm, J Hz, DMSO-d6), **δ**C =165.29 (C=O,C_1, benzohydrazide), **δ**C=163.03 (C=O, C_2, isatin), **δ**C=162.02 (C_3, C=N), **δ**C=153.25 (C_4, C-OH), **δ**C=152.59 (C_5, C-CONH), **δ**C=144.43 (C_6, C-NH, isatin) and **δ**C_7-C_{19} = 142.97 -111.37 (Aromatic ring carbons). The mass spectrum showed an important peak at position (m/z = 331.3). In addition: $C_{19}H_{12}N_3O_2^+$ (m/z=313.1), $C_{19}H_{17}N_2O^+$ (m/z=289.1), $C_{14}H_{20}N_3O_2^+$ (m/z=262.1), $C_{13}H_{14}N_3^+$ (m/z=212.0), $C_8H_{12}N_3O_2^+$ (m/z=182.9), $C_8H_{14}N_3^+$ (m/z=152.0), $C_6H_{14}N_3^+$ (m/z=128.0), $C_7H_7O^+$ (m/z=107.0), $C_6H_5^+$ (m/z=77.0), $C_4H_5^+$ (m/z=51.0).

2-2 Synthesis of $[Hg_2(L2)_2(\mu\text{-dppm})_2]$ Cl_4 and $[Hg(L2)(dppp)]Cl_2$ Complexes:

Heated solutions of $Na[PdCl_4]$ (0.10g, 0.3398 mmol) in 5 mL of absolute ethanol and the ligand (L) (0.1070g, 0.3398 mmol) in 7 mL of absolute ethanol were combined. The resulting mixture was then refluxed. After an hour, an equivalent of Phosphines (dppm and dppp) (0.3398 mmol) was added to the mixture in 5 mL of absolute ethanol. The mixture was stirred for three hours at room temperature. The mixture was then separated, resulting in a precipitate. This precipitate was filtered, washed with cold ethanol, and dried under vacuum.

$[Hg_2(L2)_2(\mu\text{-dppm})_2]Cl_4$ (1). A dark-yellow solid, yield (0.255g, 80.56%). (Melting point 269-271 ° C). IR (KBr, cm^{-1}): 3456.20m υ (O-H), 3253.69m υ(N-H), 3055.03(C-H) aromatic, 2889.17 (ν C-H), 1695.31s(C=O), 1662.52s (C=O), 1623.95sh (C=N), 1433.01s υ(Ph-P), 684.68, 1099.35s ν(C-P), 511.10s (Hg-N), 462.88s (Hg-O); ^{31}P-{^{1}H}NMR (δppm, DMSO-d6), **δ**P= 22.65(s); ^{1}H-NMR (δ ppm, J Hz, DMSO-d6), **δ**H=14.55 (s,1H, OH), **δ**H=11.77 (s, 1H, NH_{amid}), **δ**H=11.20 (s, 1H, NH_{isatin}), **δ**H=8.71 (s, 1H, H_e), **δ**H=8.02 (d, $^3J_{H\text{-}H}$=8.26 Hz,1H,H_f), **δ**H=7.91 (m, 8H, H_b, H_c, H_g, H_j, and 4H-Ph,), **δ**H=7.77 (d, $^3J_{H\text{-}H}$=8.36Hz, 1H, H_i), **δ**H = 7.63 (d, $^3J_{H\text{-}H}$ = 7.53Hz, 1H, H_a), **δ**H = 7.53 and 7.38 (m, 16H, H-Ph and 3Ph), δH = 7.11 ppm (t,$^3J_{H\text{-}H}$ = 7.66 Hz, 1H,H_h), δH = 6.95 ppm (d,$^3J_{H\text{-}H}$ = 7.79 Hz,1H, H_d), **δ**H= 5.21 (s, 2H, CH_2, dppm). Λ ($\Omega^{-1}.cm^2.mol^{-1}$): 27.58.

$[Hg(L2)(dppp)]Cl_2$ (2). A light-yellow solid, yield (0.348g, 95.72%). (Melting point 269-271 ° C). IR (KBr, cm^{-1}): 3510.20m υ (O-H), 3253.69m υ(N-H), 3053.11(C-H) aromatic 2906.53 (νC-H), 1695.31s (C=O), 1662.52s (C=O), 1623.95sh (C=N), 1433 υ(Ph-P), 692.40, 1101.28 ν(C-P), 520.74s (Hg-O), 462.88s (Hg-O); ^{31}P-{^{1}H}NMR (δppm, DMSO-d6), **δ**P=26.82(s); ^{1}H-NMR (δ ppm, J Hz, DMSO-d6), **δ**H=14.54 (s,1H, OH), **δ**H=11.72 (s, 1H, NH_{amid}), **δ**H=11.18 (s, 1H, NH_{isatin}), **δ**H=8.71 (s, 1H, H_e), **δ**H=8.02 (d, $^3J_{H\text{-}H}$ = 8.09 Hz,1H,H_f), **δ**H=7.78, 7.53 and 7.37 (m, 26H, H_h, H_c, H_a, , H_i, H_g, Hj, and 4Ph, respectively), **δ**H=7.11 (t, $^3J_{H\text{-}H}$=7.41 Hz,1H,H_b), **δ**H=6.95 (d, $^3J_{H\text{-}H}$=7.57 Hz, 1H, H_d), **δ**H= 2.98 (s, 4H, $2CH_2$ alph., terminal, dppp) **δ**H= 1.94 (s, 2H, CH_2 alph., moderation, dppp). Λ ($\Omega^{-1}.cm^2.mol^{-1}$): 22.50.

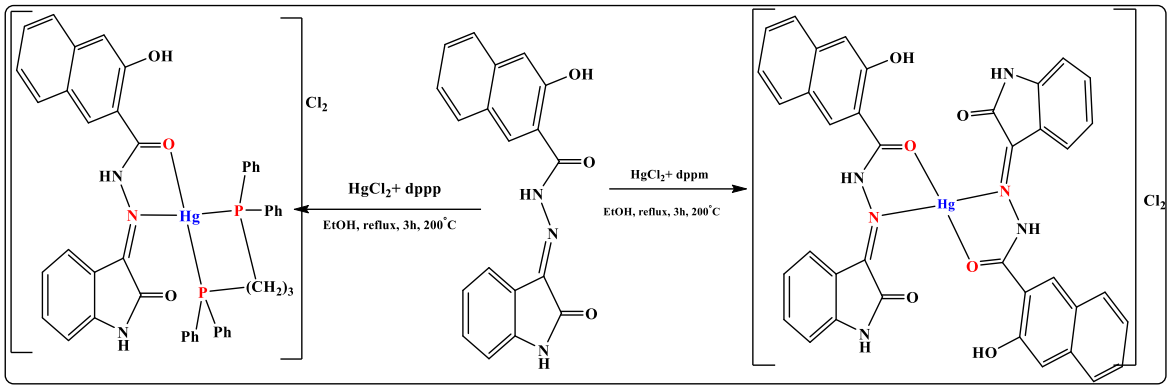

Figure (1): Preparation of complexes.

3. Results and Discussion

Analysis of the conductivity measurements showed that complexes 1 formed in a 2:2:2 ratio (mercury ion: Ligand L: dppe), whereas complexes 2 formed in a 1:1:1 ratio (mercury ion: Ligand L: dppp). The methods used to synthesise these mixed-ligand complexes yielded materials of high purity, as confirmed by analysis. These complexes were only slightly soluble in methanol, ethanol, and acetone, but fully soluble in DMF and DMSO. Despite testing various solvents and recrystallisation techniques, all attempts to obtain suitable crystals for crystallographic analysis were unsuccessful.

The molar conductivity of the prepared complexes was measured in DMSO at 25°C at a concentration of 10^{-3} mol/L. All complexes (1 and 2) exhibited values 27.58 to 22.50 $\Omega^{-1}\cdot cm^2\cdot mol^{-1}$ respectively, indicating that they are 1:2 electrolytes[32], [33]. This suggests that complexes (1 and 2) have two chloride ions positioned outside the coordination sphere.

The IR spectrum of the prepared ligand showed characteristic vibration bands at 1697 cm^{-1} and 1664 cm^{-1}, indicating the presence of (C=O) groups. It also displayed a band at 1625 cm^{-1} related to the (C=N) group, a band at 3411 cm^{-1} related to the (O-H) group, and a band at 3247 cm^{-1} assigned to the (N-H) group [20], [21]. Complexes (1 and 2) displayed absorption bands within the ranges of 1695cm^{-1} and 1662 cm^{-1} for carbonyl (C=O) groups. The hydroxyl (O-H) group showed bands within 3456-3510 cm^{-1}, the amine (N-H) group showed bands 3253 cm^{-1}, and the nitrile (C=N) group appeared at1625 cm^{-1}. Along with two distinct bands at 742 and 744 cm^{-1} attributed to the bending vibration of phenyl (C-H) groups. The absorption bands of phosphinates in complexes (1 and 2) appeared within 1433cm^{-1}, related to the phenylphosphine (Ph-P) group. Two distinctive bands were observed at 1099-1101 cm^{-1} and 684-692 cm^{-1}, associated with vibrational modes. Additionally, absorption bands of (C-H) groups were observed within (2889-2906cm^{-1}),[20], [21], as shown in Figure (1) and Figure (2).

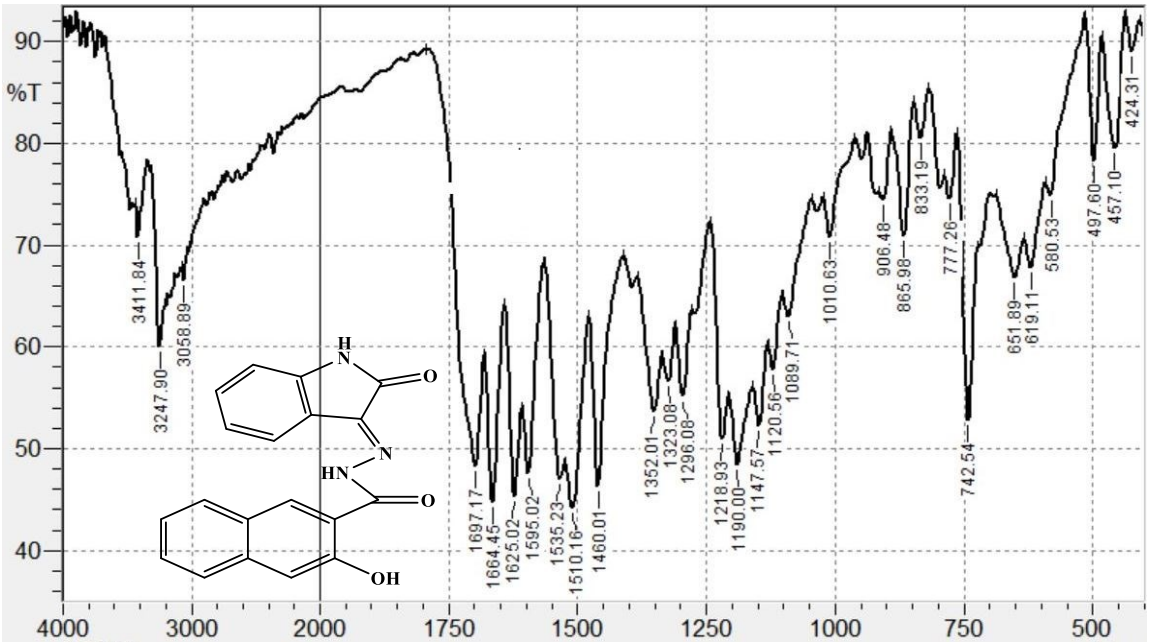

Figure (2): FT-IR of (L) ligand

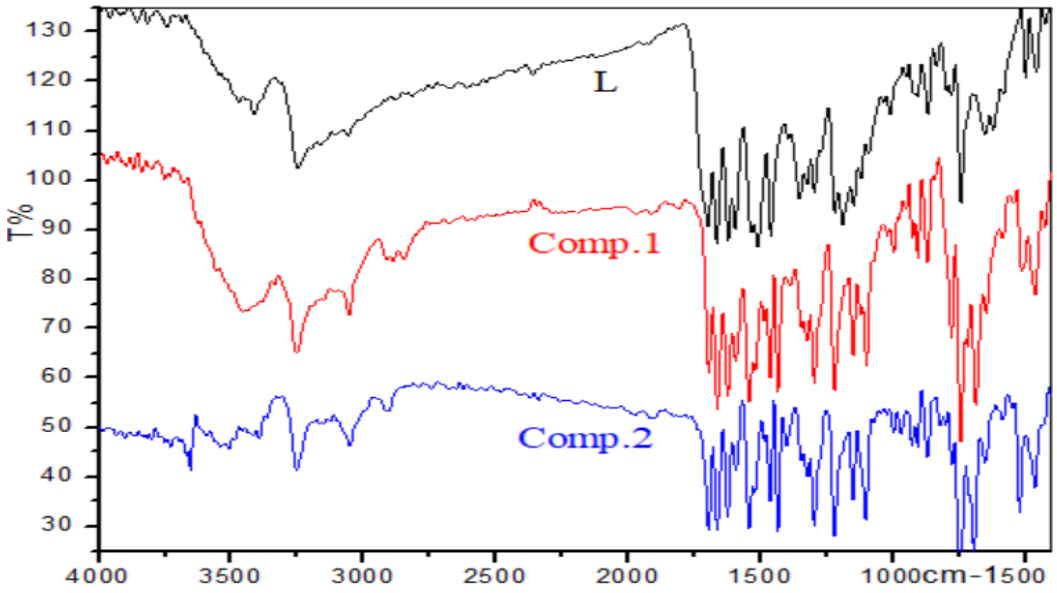

Figure (3): FT-IR of all compounds

Figure 3 shows the ^{1}H-NMR spectrum of the ligand. It features a singlet at δH = 14.54 ppm (OH proton), a singlet at δH = 11.78 ppm (NH_{amid}), a singlet at δH = 11.20 ppm ($NH_{istatin}$), a doublet at δH = 8.02 ppm (H_f, $^{3}J_{H-H}$ = 8.24 Hz), a doublet at δH = 7.77 ppm (H_i, $^{3}J_{H-H}$ = 8.36 Hz), and a doublet at δH = 7.63 ppm (H_a, $^{3}J_{H-H}$ = 7.59 Hz). Additionally, there's a triplet at δh = 7.53 ppm (H_c, $^{3}J_{H-H}$ = 7.59 Hz), a multiplet at δH = 7.38 ppm (H_j, H_g and H_h), a triplet at δH = 7.11 ppm (H_b, $^{3}J_{H-H}$ = 7.47 Hz), and a doublet at δH = 6.94 ppm (H_d, $^{3}J_{H-H}$ = 7.76 Hz).

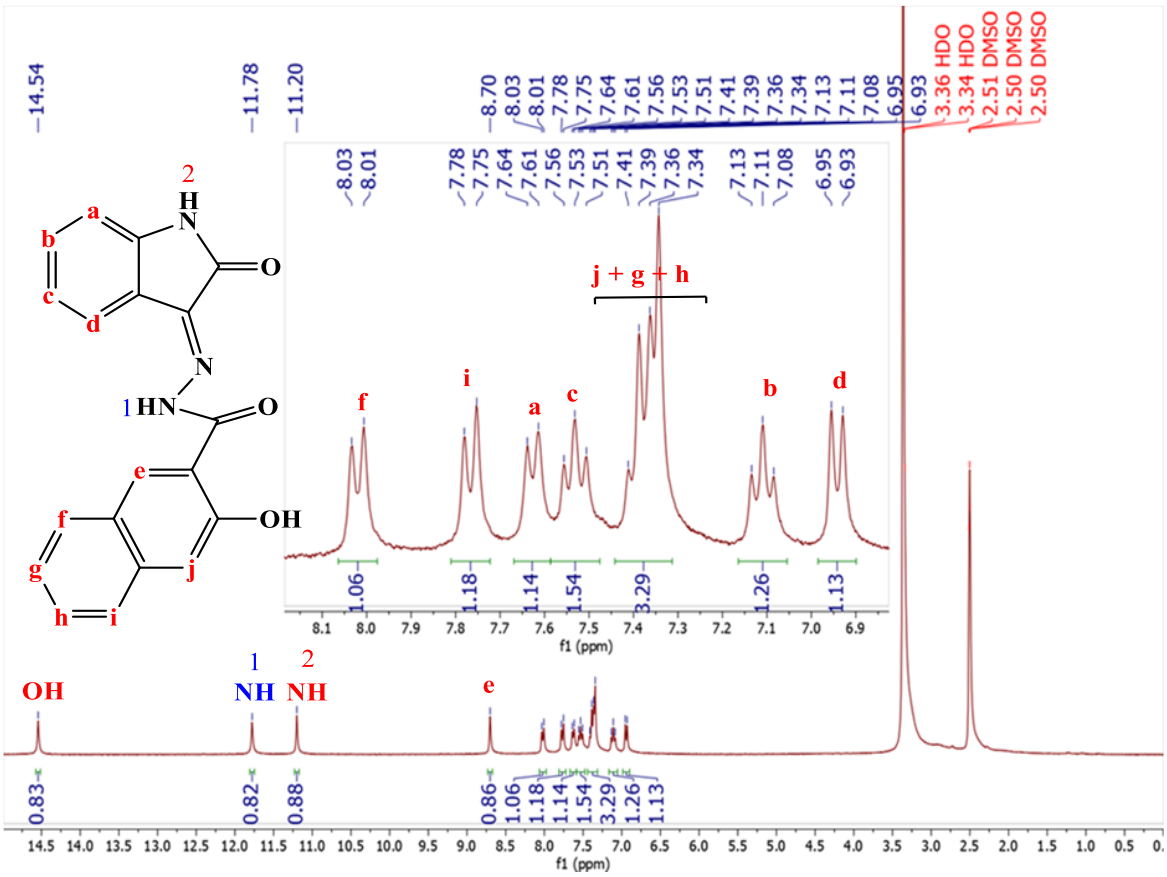

Figure (4): ^{1}H-NMR of the (L) ligand

The ^{13}C-NMR spectrum of the ligand (L) displayed signals at δC=165.29ppm and δC=163.03ppm, corresponding to the (C=O) carbons in the benzoyl and isatin groups, respectively. Signals were also observed in the range of δC=162.02-144.43ppm for atoms C_3, C_4, C_5, and C_6 in sequence, and in the range δC=142.97-111.37ppm attributed to the carbons C_7-C_{19} for CPh, as shown in Figure 4.

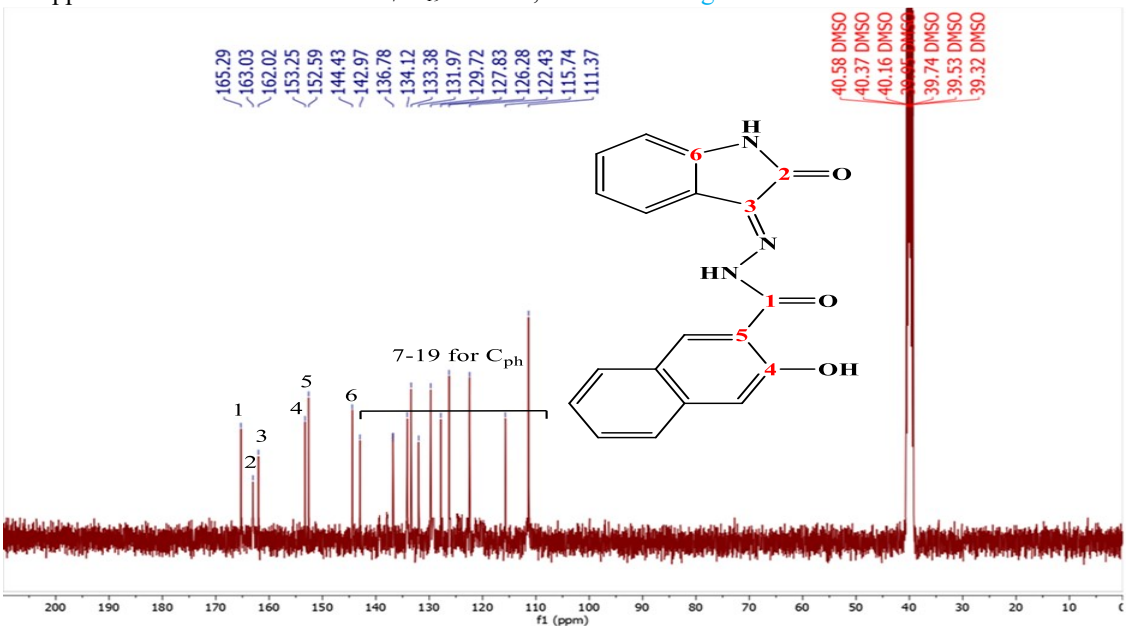

Figure (5): ^{13}C-NMR of the (L) ligand

Mass spectrum analysis of the ligand (L) showed multiple bands at various positions, with a notable peak at (m/z = 331.3) corresponding to the mass of the ligand $C_{19}H_{13}N_3O_3$, as illustrated in Figure (5). Additionally, the spectrum revealed distinct bands that were compared against theoretical and practical calculations for each peak, corresponding to specific components of the molecular formula, as shown in Scheme (2), as follows: $C_{19}H_{13}N_3O_3^{+\cdot}$ (m/z=331.3), $C_{19}H_{20}N_3^{+}$ (m/z=290.17), $C_{13}H_{13}N_2O^{+}$ (m/z=213.1), $C_{10}H_{20}N_3^{+}$ (m/z=182.17), $C_{10}H_{18}N^{+}$ (m/z=152.14), $C_5H_{10}N_3O^{+}$ (m/z=128.08), $C_7H_{10}N^{+}$ (m/z=108.08), $C_6H_5^{+}$ (m/z=77.04), CH_2Cl^{+} (m/z=48.98).

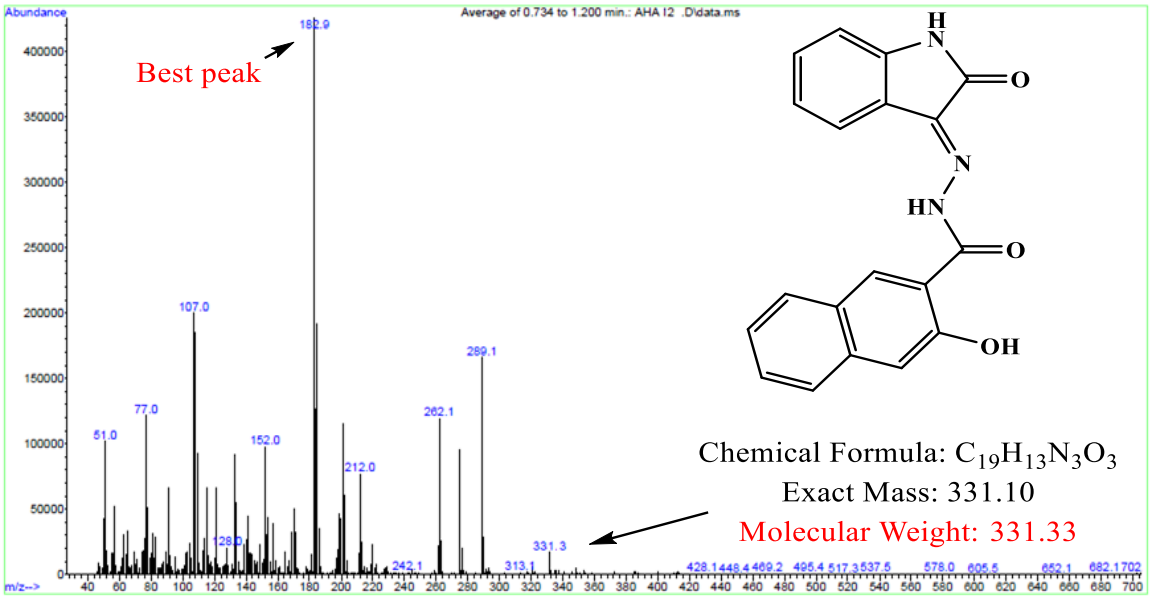

Figure (6): Mass spectrum of the first ligand (L1)

^{1}H-NMR spectra of complex 1 showed diverse signals for both the ligand (L) and the corresponding phosphine, with a 1:1 integration ratio, confirming the proposed structures. The ^{1}H NMR spectrum of complex 2 showed diverse signals for both ligands (L) and the corresponding phosphine, with a 2:2 integration ratio, supporting the proposed structure. The spectra of complexes 1and 2 displayed distinctive signals for the coordinated phosphine groups.

^{1}H-NMR spectrum of complex (1) showed a singlet at (δH = 14.55 ppm) and with the integration of one proton attributed to the proton of the OH group, a singlet at (δH = 11.77 ppm) and with the integration of one proton attributed to the proton of the NH_{amid} group and singlet at (δH = 11.20 ppm) and with the integration of one proton attributed to the proton of the NH_{isatin} group, a singlet at (δH = 8.71 ppm) attributed to the H_e proton, a doublet signal at (δH = 8.02 ppm) with a coupling constant ($^{3}J_{H-H}$ = 8.26 Hz) by integration of one proton it is due to the H_f proton, one big signals centered at (δH = 7.91 ppm) with the integration of 8 protons attributed to the protons of H_b, H_c, H_g, H_j, and 4H-Ph, and a doublet signal at (δH = 7.77 ppm) with a coupling constant ($^{3}J_{H-H}$ = 8.36 Hz) By integration of one proton it is due to the H_i proton, and a double signal at (δH = 7.63 ppm) with a coupling constant ($^{3}J_{H-H}$ = 7.53 Hz) by integration of one proton it is due to the H_a proton, one big multicentric signals centered at (δH = 7.91 ppm) with the integration of 8 protons attributed to the protons of H_b, H_c, H_g, H_j, and 4H-Ph, and binary multicentric signals, the first at (δH = 7.53 ppm) and the second at (δH = 7.38 ppm), with 16 protons integration attributed to the H-Ph, and 3Ph, and a triplet signal at (δH = 7.11 ppm) with a coupling constant ($^{3}J_{H-H}$ = 7.66 Hz) by integration of one proton it is due to the H_h proton, and a doublet signal at (δH = 6.95 ppm) with a coupling constant ($^{3}J_{H-H}$ = 7.79 Hz) by integration of one proton it is due to the H_d proton, and he also showed the presence of a singlet at (δH = 5.21 ppm) and by integration of two protons it is due to the (CH_2) group in the dppm ligand in the complex.

^{1}H-NMR spectrum of complex (2), as shown in Fig. 6, Showed a singlet at (δH = 14.54 ppm) with one proton integration attributed to the OH proton, the two singlet signals appeared at (δH=11.72ppm, 1H) and (δH=11.18ppm, 1H), corresponding to the NH protons in the hydrazone and isatin groups, respectively, a singlet at (δH = 8.71 ppm) attributed to the H_e proton, a doublet signal at (δH = 8.02 ppm) with a coupling constant ($^{3}J_{H-H}$ = 8.09 Hz) by integration of one proton it is due to the H_f proton, and three multicentric signals, the first at (δH = 7.78 ppm), the second at (δH = 7.53 ppm), and the third at (δH = 7.37 ppm) with 26 protons integration attributed to the H_h, H_c, H_a, H_i, H_g, H_j, and 4Ph, a triplet signal at (δH = 7.11 ppm) with a coupling constant ($^{3}J_{H-H}$ = 7.41 Hz) with one proton integration attributed to the H_b proton, in addition to a binary signal at (δH = 6.95 ppm) with a coupling constant ($^{3}J_{H-H}$ = 7.57 Hz) attributed to the H_d proton.

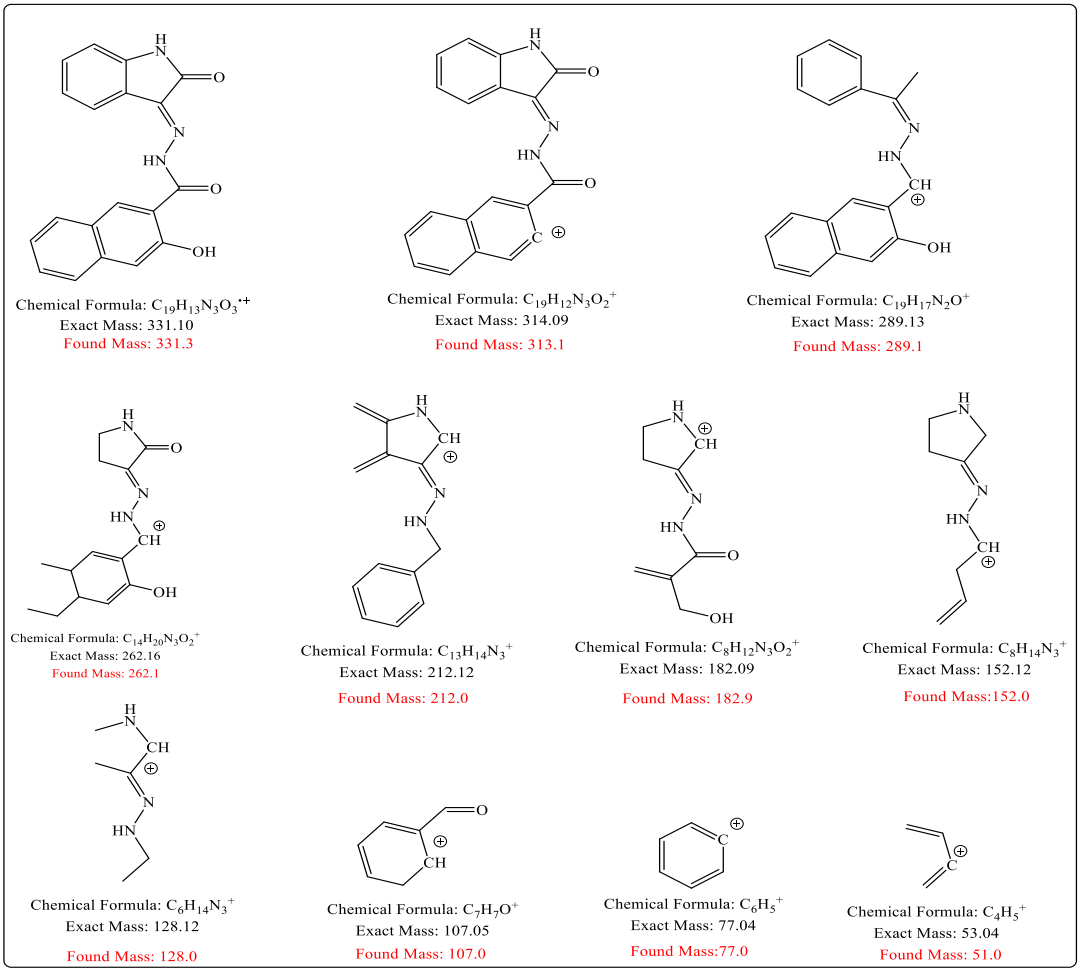

Figure (7): Possible fragmentation of the first ligand (L1)

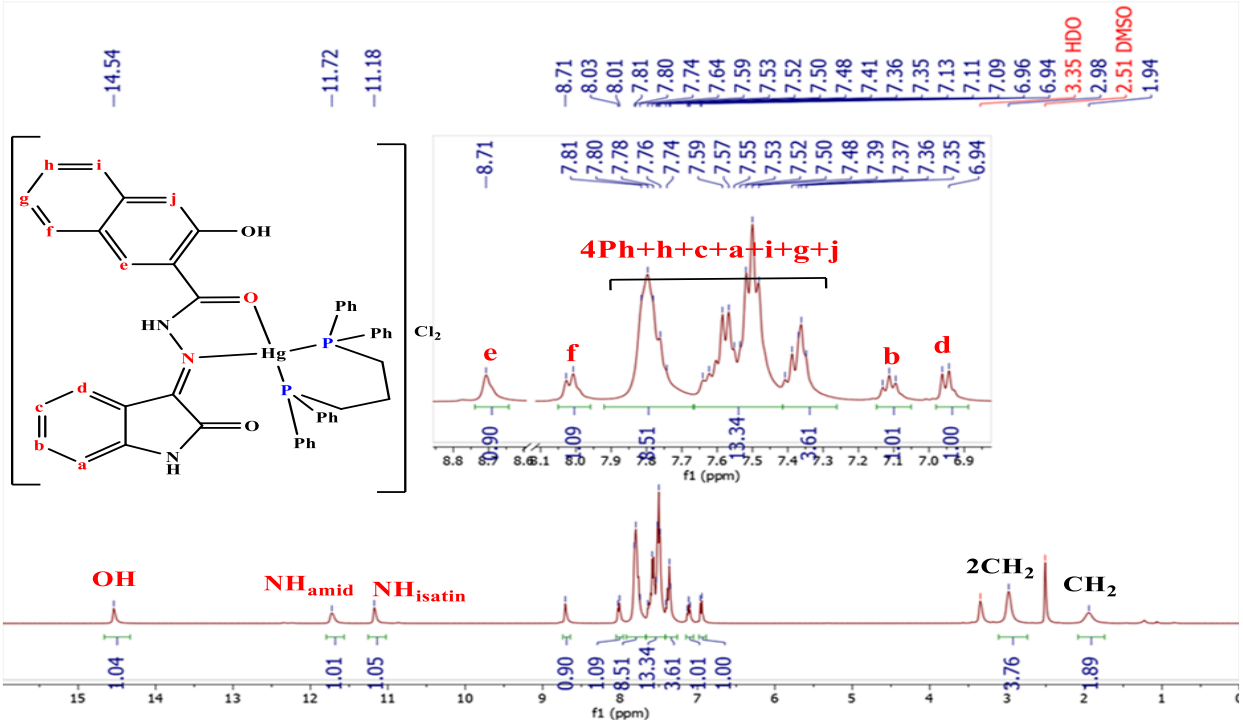

Figure (8): ^{1}H-NMR of the [Hg(L2)dppp]Cl_2

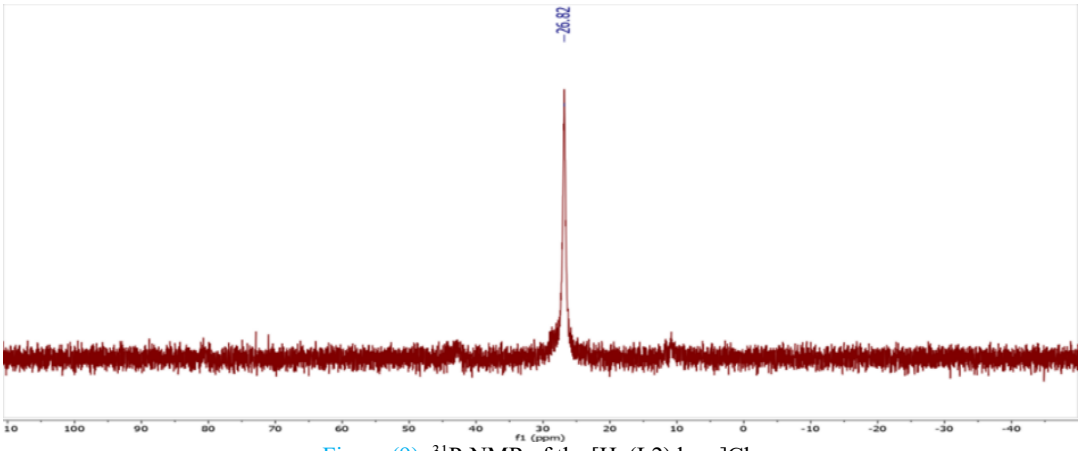

Figure (9): ^{31}P-NMR of the [Hg(L2)dppp]Cl_2

Signals due to (CH_2) groups were observed at (δH= 5.21ppm, s, 2H, CH_2) in dppm, two signals were found at (δH=2.98ppm, s, 4H, $2CH_2$) and (δH=1.94ppm, s, 2H, CH_2) for dppp.
^{31}P-{1H}NMR spectrum of the complex (1) displayed a singlet at (δP = 22.65ppm) with Mercury satellites. This positive value reflects the bridging role of the dppm ligand in the complex[22]. This also supports the proposed bridging coordination between the oxygen, nitrogen, and phosphorus atoms of the ligand (L) with Mercury.

^{31}P-{1H}NMR spectrum of the complex (2) exhibited a singlet at (δP=26.82ppm) with Mercury satellites. This singlet suggests the equivalent nature of the phosphorus atoms in the dppp ligand, which coordinates in a chelating bidentate manner with Mercury[34]. Additionally, it implies the presence of two equivalent atoms in trans positions to the phosphorus atoms, forming a square-planar geometry around the platinum ion. This also supports the proposed bridging coordination between the oxygen, nitrogen, and phosphorus atoms of the ligand (L) with Mercury.

Recent SEM studies on the geometrical structure of coordination complexes have demonstrated the potential to produce regularly structured geometries at the nanoscale [35]. Preparing Nano compounds uses methods similar to those used for complexes. This includes using small amounts of coordinating ligands and metal salts, with the components added gradually[36].

SEM analysis of complex (1) depicted in Fig. 8 was conducted using a 1µm (100nm) cross-sectional area and a magnification power of MAG: 30.0 KX. The half-diameters indicated in the Gaussian fit curve were 145.42607nm, representing nanoscale particles of the complex.

The SEM analysis of the complex (2) depicted in Fig. 9 was performed using a 500 nm cross-sectional area and a magnification power (MAG: 50.0 kX). The semi-major diameters obtained from the Gaussian Fit curve indicated a peak semi-major diameter for complex particles of 142.87278nm. These findings are significant in coordination chemistry because they suggest potential for using these complexes in various applications. Besides the results presented here, measurements have confirmed the formation of regular nanostructures with high porosity, indicating their suitability for uses that demand a large surface area and porosity, such as hydrogen storage[37], [38].

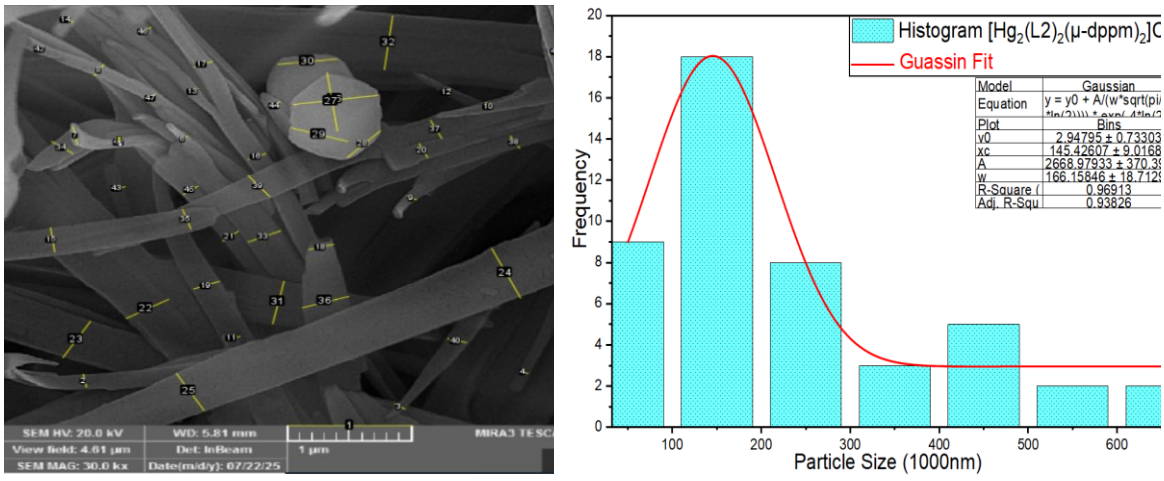

Figure (10): SEM images of the complex 1 and Histogram for the distribution of particle size along with Gaussian fit

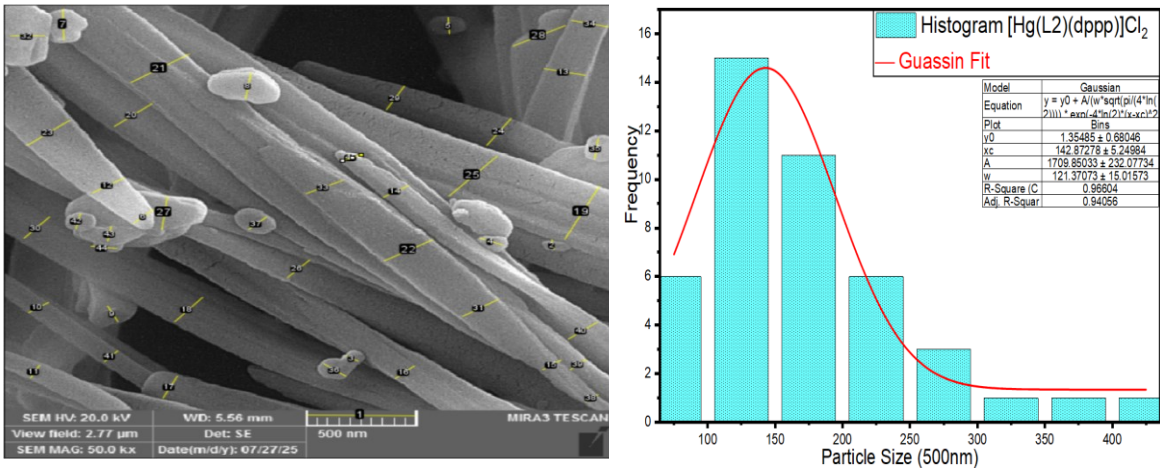

Figure (11): SEM images of the complex 2 and Histogram for the distribution of particle size along with Gaussian fit

The XRD results for the powders of some studied complexes showed that they are crystalline, with crystallinity degrees ranging of complex 1 and 2 (23.49% and 28.06%) respectively, as shown in Table 1. This was determined by calculating the ratio of the area under the crystalline peaks (Ac) to the total area (Ac+Aa), where (Aa) represents the area under the baseline. The analysis was performed using Origin 2025b.

Table 1. The Total Area under the Crystalline Peaks and Crystallinity Degree of prepared complexes

Complexes	Total Area under the Crystalline (Ac) Peak	Total Area (Ac+Aa)	% Crystallinity Degree [Ac/Ac+Aa]
(1)	1094.64431	4659.63369	23.49
(2)	1365.73632	4866.29538	28.06

The results also showed that the crystallite size ranged from 8.27 to 183.47 nm, confirming the SEM findings that these complexes contain nanosized particles within their crystalline structures, whether appearing as clusters, rods, or nanocrystals. Fig. 10 displays the XRD patterns of the prepared complexes.

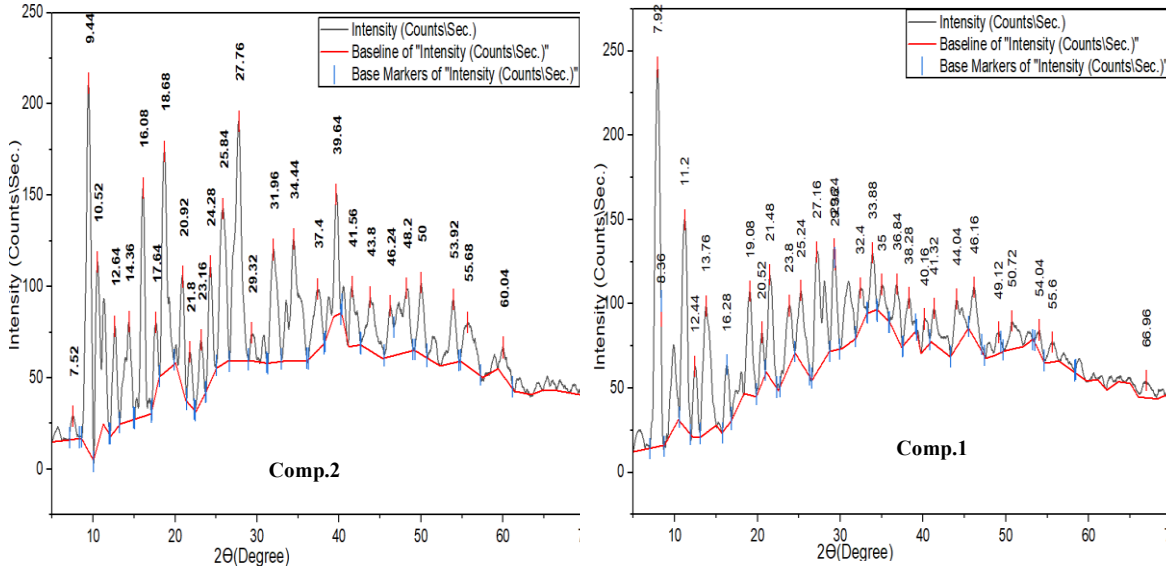

Figure (12): The XRD for the prepared complexes (1 and 2)

Thermal analysis (TGA) was performed on Mercury (II) complexes across a temperature range of 30-800 °C, as shown in Fig. 11. The TGA curves indicate the presence of either outside water molecules, coordinated water, or both, along with anions that are part of the Complexes' coordination sphere[39].

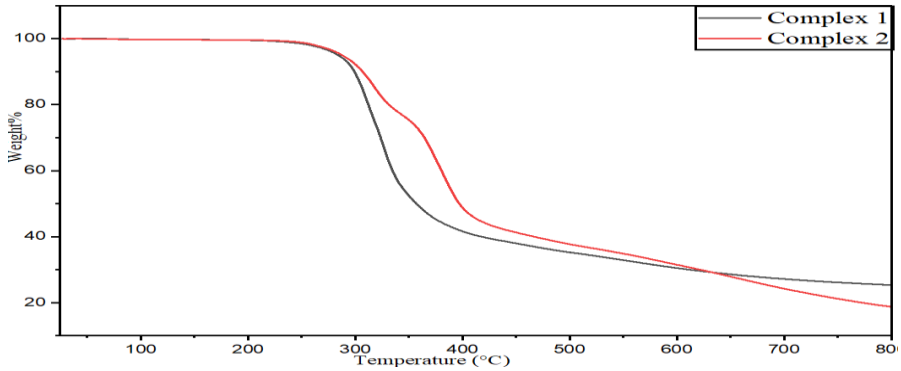

Figure (13): The TGA for the prepared complexes (1 and 2)

Table 2 shows the temperature ranges and the corresponding percentage of mass loss for the Mercury (II) complexes. The observed weight loss from experiments aligns well with the values predicted theoretically.

Table (2): Data of the thermogravimetric analysis curve of some prepared complexes.

Complexes	Step	T_i/°C	T_f/°C	T_{DTG} max	Weight mass loss %		Reaction	Total mass loss%
					Cal.	Found		
$[Hg_2(L2)_2(\mu\text{-dppm})_2]Cl_4$	1	84.28	412.51	248.39	58.90	58.97	$C_{52}H_{64}Cl_4N_6O_4P_4$	77.45 found
	2	412.51	583.76	498.13	8.33	8.61	13C	
	3	583.76	808	695.88	9.62	9.87	15C	76.85 Cal.
							2HgO	
$[Hg(L)(dppp)]Cl_2$	1	277.71	383.58	330.64	49.09	49.18	$C_{21}H_{39}Cl_2N_3O_2P_2$	78.78 found
	2	383.58	559.37	471.47	11.83	11.89	10C	
	3	559.37	808	683.68	17.74	17.71	15C	78.66 Cal.
							HgO	

For complex 1, the initial stage between 84.28-412.51°C involves losing a $C_{52}H_{64}Cl_4N_6O_4P_4$ molecule, resulting in a 58.97% mass loss (calculated = 58.90%). The second stage, between 412.51-583.76°C, involves losing 13C, with a mass loss of 8.61% (calculated = 8.33%). The third stage, from 583.76 to 808 °C, involves the decomposition of 15C, with a mass loss of 9.87% (calculated to be 9.62%). After this, two molecules of mercury oxide remain as a metallic residue, constitutes 77.45% of the remaining mass (calculated = 76.85%)[40], [41], [42]. Where complex 2 loses mass in the first stage within 277.71-383.58°C, aligning with the loss of $C_{21}H_{39}Cl_2N_3O_2P_2$ molecules and a mass reduction of 49.18% (calculated as 49.09%). The second decomposition occurs between 383.58-559.37°C, involving a significant mass loss, represented by 10C, which amounts to 11.89% (calculated as 11.83%). The final stage occurs between 559.37-808 °C, characterized by the loss of 15C and a mass loss of 17.71% (calculated as 17.74%). Mercury oxide remains as the final residue, accounting for 21.22% (calculated as 21.34%). All complexes showed high activity against *Staphylococcus aureus* and *Pseudomonas aeruginosa*, except for the ligand with strong and weak inhibition[43].

The antibacterial activity of the tested compounds was evaluated against Staphylococcus aureus and Pseudomonas aeruginosa using the agar well diffusion method at concentrations of 100 mg/ml and 50 mg/ml. The results consistently revealed a higher level of inhibition against S. aureus compared to *P. aeruginosa* across almost all samples. Specifically, the inhibition zones for *S. aureus* ranged between 0 mm to 37 mm, while for *P. aeruginosa* they were generally smaller, ranging from 0 mm and 17 mm. as shown in Chem. (3).

This variation in susceptibility can be attributed to fundamental structural and physiological differences between the two bacterial species. Staphylococcus aureus is a Gram-positive bacterium, characterized by a thick peptidoglycan layer in its cell wall and the absence of an outer membrane. This makes it generally more permeable to antimicrobial agents. In contrast, Pseudomonas aeruginosa is a Gram-negative bacterium with an additional outer membrane that acts as a strong permeability barrier. This outer membrane, along with its efflux pumps and enzymatic resistance mechanisms, significantly reduces the penetration and retention of many antibacterial compounds. Therefore, it needs extensive future study at other specific concentrations of complexes[43], [43].

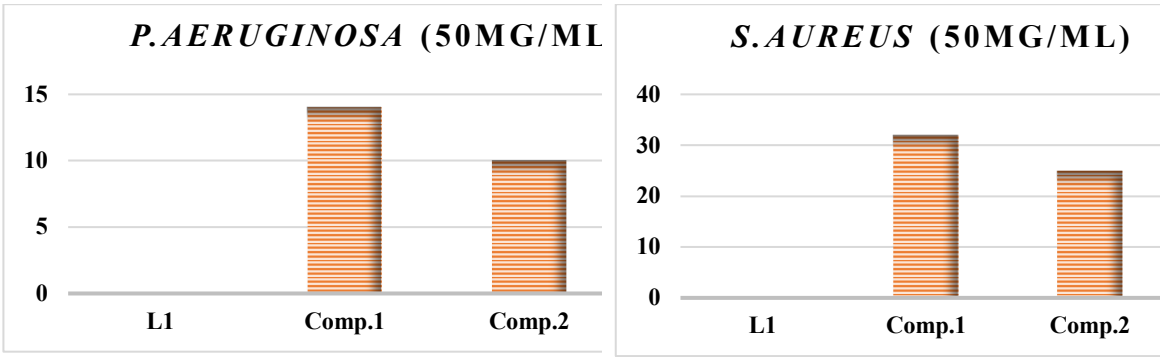

Schem 3: Biological activity of the prepared compounds at 50mg/ml against bacteria.

Table (3): Biological activity of the prepared compounds against bacteria.

	S. aureus		*P. aeruginosa*	
Comp.	100 mg/ml	50 mg/ml	100 mg/ml	50 mg/ml
(L1)	0 mm	0 mm	0 mm	0 mm
(1)	37mm	32 mm	17 mm	14 mm
(2)	25 mm	25 mm	14 mm	10 mm

CONCLUSIONS

The new Hg(II) complexes were synthesised with the ligand (E)-3-hydroxy-N'-(2-oxoindolin-3-ylidene)-2-naphthohydrazide (L) with other mixed ligands; the proposed formulas were $[Hg_2(L2)_2(\mu\text{-dppm})_2]Cl_4$ and $[Hg(L_2)(dppp)]Cl_2$. The ligands (dppm) are coordinated as bridging ligands in binuclear complexes, while (dppp) acts as a bidentate chelating ligand in dinuclear complexes. The prepared complexes were characterized using molar conductivity measurements, FT-IR spectroscopy, ^{1}H, ^{13}C, Mass, and ^{31}P-NMR spectroscopy. The results of the SEM examination showed that the studied complexes had Nano scale sizes ranging from (142.87278- 145.42607nm), it has nanocrystalline structures and aggregates, and this was confirmed by XRD analysis, where the studied complexes gave an average nanoscale size about (8.27 to 183.47nm) and a degree of crystallinity ranging between (23.49% and 28.06%). This was confirmed by the gravimetric TG, which indicates the stability of the complexes at normal temperatures, while they disintegrate in stages into other components, including palladium oxide. All the prepared compounds showed high activity against *Staphylococcus aureus*, except for the ligand, at both concentrations.

REFERENCES

[1] Miroslaw, B. Homo- and Hetero-Oligonuclear Complexes of Platinum Group Metals (PGM) Coordinated by Imine Schi ff Base Ligands work of. (2020).

[2] Saritha, T. J. & Metilda, P. Synthesis, spectroscopic characterization and biological applications of some novel Schiff base transition metal (II) complexes derived from curcumin moiety. *J. Saudi Chem. Soc.* 25, 101245 (2021). doi: 10.1016/j.jscs.2021.101245.

[3] Vigato, P. A. & Tamburini, S. The challenge of cyclic and acyclic schiff bases and related derivatives. *Coord. Chem. Rev.* 248, 1717–2128 (2004). doi: 10.1016/j.cct.2003.09.003.

[4] Pathak, A., Soni, N., Pandey, D. D. & Verma, D. Recent Advances, Future Challenges, Sar And Antimicrobial Activities Of Isatin: A Breaf Review. *J. Pharm. Negat. Results* 13, 7285–7307 (2022). doi: 10.47750/pnr.2022.13.S09.856.

[5] Pandeya, S. N., Smitha, S., Jyoti, M. & Sridhar, S. K. Biological activities of isatin and its derivatives. *Acta Pharm.* 55, 27–46 (2005).

[6] Rohini, R. *et al.* Synthesis of mono, bis-2-(2-arylideneaminophenyl) indole azomethines as potential antimicrobial agents. *Arch. Pharm. Res.* 34, 1077–1084 (2011). doi: 10.1007/s12272-011-0705-z.

[7] Akhaja, T. N. & Raval, J. P. Design, synthesis and in vitro evaluation of tetrahydropyrimidine-isatin hybrids as potential antitubercular and antimalarial agents. *Chinese Chem. Lett.* 23, 785–788 (2012). doi: 10.1016/j.cclet.2012.05.004.

[8] Ibrahim, H. S. *et al.* Isatin-pyrazole benzenesulfonamide hybrids potently inhibit tumor-associated carbonic anhydrase isoforms IX and XII. *Eur. J. Med. Chem.* 103, 583–593 (2015). doi: 10.1016/j.ejmech.2015.09.021.

[9] Meena, K. *et al.* One pot three component synthesis of spiro [indolo-3,10′-indeno[1,2-b] quinolin]-2,4,11′-triones as a new class of antifungal and antimicrobial agents. *Chinese Chem. Lett.* 28, 136–142 (2017). doi: 10.1016/j.cclet.2016.06.025.

[10] Inhibitors, T. *et al.* Dihydropyrimidinone-Isatin Hybrids as Novel Non-nucleoside HIV-1 Reverse Transcriptase Titiksh Devale (Corresponding author) Jaipur National University , Jagatpura , Jaipur , India Faculty of Pharmacy , The Maharaja Sayajirao University of Baroda , Vado. (2017).

[11] Ashraf, A. *et al.* Synthesis, Characterization, and in Silico Studies of Novel Spirooxindole Derivatives as Ecto-5′-

Nucleotidase Inhibitors. *ACS Med. Chem. Lett.* 11, 2397–2405 (2020).
[12] Bortolami, M., Leonelli, F., Feroci, M. & Vetica, F. Step Economy in the Stereoselective Synthesis of Functionalized Oxindoles via Organocatalytic Domino/One-pot Reactions. *Curr. Org. Chem.* 25, 1321–1344 (2021). doi: 10.2174/1385272825666210518124845.
[13] Baddepuri, S. *et al.* An ultrasound assisted green protocol for the synthesis of quinoxaline based bisspirooxindoles: Crystal structure analysis, enone umpolung, DFT calculations, anti-cancer activity, and molecular docking studies. *Synth. Commun.* 53, 835–854 (2023).
[14] Nivetha, N. *et al.* Benzodioxole grafted spirooxindole pyrrolidinyl derivatives: synthesis, 14, molecular docking and anti-diabetic activity. *RSC Adv.* 12, 24192–24207 (2022). doi: 10.1039/d2ra04452h.
[15] Al Furaiji, K. H. M., Al Hassani, R. A. M. & Hussein, H. H. Synthesis and Antibacterial Activity of Azomethine Ligand and Their Metal Complexes: A Combined Experimental and Theoretical Study. *Indones. J. Chem.* 24, 54–66 (2024).
[16] M. Scott, L., R. Lawrence, H., M. Sebti, S., J. Lawrence, N. & Wu, J. Targeting Protein Tyrosine Phosphatases for Anticancer Drug Discovery. *Curr. Pharm. Des.* 16, 1843–1862 (2010). doi: 10.2174/138161210791209027.
[17] El-Sonbati, A. Z. *et al.* Mixed ligand transition metal (II) complexes: Characterization, spectral, electrochemical studies, molecular docking and bacteriological application. *J. Mol. Struct.* 1248, 131498 (2022).
[18] Kyhoiesh, H. A. K. & Al-Adilee, K. J. Pt (IV) and Au (III) complexes with tridentate-benzothiazole based ligand: synthesis, characterization, biological applications (antibacterial, antifungal, antioxidant, anticancer and molecular docking) and DFT calculation. *Inorganica Chim. Acta* 555, 121598 (2023).
[19] Kyhoiesh, H. A. K. & Al-Adilee, K. J. Synthesis, spectral characterization, antimicrobial evaluation studies and cytotoxic activity of some transition metal complexes with tridentate (N, N, O) donor azo dye ligand. *Results Chem.* 3, 100245 (2021).
[20] Pakravan, P., Kashanian, S., Khodaei, M. M. & Harding, F. J. Biochemical and pharmacological characterization of isatin and its derivatives: From structure to activity. *Pharmacol. Reports* 65, 313–335 (2013).
[21] Ali, A. Q., Teoh, S. G., Eltayeb, N. E., Ahamed, M. B. K. & Majid, A. A. Synthesis of nickel(II) complexes of isatin thiosemicarbazone derivatives: In vitro anti-cancer, DNA binding, and cleavage activities. *J. Coord. Chem.* 67, 3380–3400 (2014). doi: 10.1080/00958972.2014.959943.
[22] Singh, V. *et al.* Recent developments on the potential biological applications of transition metal complexes of thiosemicarbazone derivatives. *Polyhedron* 245, 116658 (2023).
[23] Zhong, W. *et al.* Syntheses, characterization of Ni (II)/Zn (II) complexes derived from flexible tricarboxylate ligand and 2, 2′-bipyridine and their methyl violet dye photodegradation applications. *J. Mol. Struct.* 1287, 135718 (2023).
[24] Masoud, M. S., Soayed, A. A., Almesmari, S. A. & Elsamra, R. M. I. New Mixed-Ligand Complexes of Cytosine and Its Silver Nanoparticles: Spectral, Analytical, Theoretical and Biological Activity Studies. *J. Inorg. Organomet. Polym. Mater.* 31, 2842–2858 (2021). doi: 10.1007/s10904-021-01945-y.
[25] Sumrra, S. H. *et al.* Coordination behavior, structural, statistical and theoretical investigation of biologically active metal-based isatin compounds. *Chem. Pap.* 76, 3705–3727 (2022). doi: 10.1007/s11696-022-02123-1.
[26] Khalil, A. & Adam, M. S. S. Bimetallic bis-Aroyldihydrazone-Isatin Complexes of High O=V(IV) and Low Cu(II) Valent Ions as Effective Biological Reagents for Antimicrobial and Anticancer Assays. *Molecules* 29, (2024). doi: 10.3390/molecules29020414.
[27] Symes, D. L. G. & Masuda, J. D. Recent advances in heavier group 15 (P, As, Sb, Bi) radical chemistry - frameworks, small molecule reactivity, and catalysis. *Dalt. Trans.* 54, 5234–5249 (2025).
[28] Kainat, S. F. *et al.* Recent developments in the synthesis and applications of terpyridine-based metal complexes: a systematic review. *RSC Adv.* 14, 21464–21537 (2024). doi: 10.1039/d4ra04119d.
[29] Werra, J. A. *et al.* Effective Control of the Electron-donating Ability of Phosphines by using Phosphazenyl and Phosphoniumylidyl Substituents. *Zeitschrift fur Anorg. und Allg. Chemie* 646, 794–799 (2020). doi: 10.1002/zaac.202000028.
[30] Parewa, R. K., Yadav, H., Saini, A. K., Dadheech, S. & Scholar, R. Synthesis of Zinc(II), Mercury(II), And Iron(III) Complexes, Their Characterization Techniques And Applications. 12, 730 (2024).
[31] Killian, L., Bienenmann, R. L. M. & Broere, D. L. J. Quantification of the Steric Properties of 1,8-Naphthyridine-Based Ligands in Dinuclear Complexes. *Organometallics* 42, 27–37 (2023). doi: 10.1021/acs.organomet.2c00458.
[32] Marciniec, B., Pietraszuk, C., Pawluć, P. & MacIejewski, H. Inorganometallics (Transition Metal-Metalloid Complexes) and Catalysis. *Chem. Rev.* 122, 3996–4090 (2022). doi: 10.1021/acs.chemrev.1c00417.
[33] Khalid Farhan, L. & Yassien Khuder, H. The Role of Transition Metal Complexes in Catalysis: Mechanisms and Industrial Applications INTRODUCTION TO TRANSITION METAL COMPLEXES. *Eur. J. Appl. Sci. Eng. Technol.* 3, 132–157 (2025). doi: 10.59324/ejaset.2025.3(4).13.
[34] Jebour, I. K., Mohammed, M. Y. & Alheety, M. A. Synthesis and Characterization of Novel Nano Dithiocarbamate Complexes Derived From GO-benzimidazole. *Diyala J. Pure Sci.* 12, 108–121 (2016).
[35] Malinowski, J., Zych, D., Jacewicz, D., Gawdzik, B. & Drzeżdżon, J. Application of coordination compounds with transition metal ions in the chemical industry—a review. *Int. J. Mol. Sci.* 21, 1–26 (2020). doi: 10.3390/ijms21155443.
[36] Salih, B. D., Alheety, M. A., Mahmood, A. R., Karadag, A. & Hashim, D. J. Hydrogen storage capacities of some

new Hg (II) complexes containing 2-acetylethiophene. *Inorg. Chem. Commun.* 103, 100–106 (2019).
[37] Al-Janabi, A. S. M., Al-Samrai, O. A. Y. & Alheety, M. A. Novel Mercury(II) 1-Phenyl-1H-tetrazol-5-thiol and carbon nanotube complexes: synthesis, characterization and H2 storage capacities. *Chem. Data Collect.* 28, 100399 (2020). doi: 10.1016/j.cdc.2020.100399.
[38] Al-Nassiry, A. I. A., Al-Janabi, A. S. M., Thayee Al-Janabi, O. Y., Spearman, P. & Alheety, M. A. Novel dithiocarbamate–Hg(II) complexes containing mixed ligands: Synthesis, spectroscopic characterization, and H2 storage capacity. *J. Chinese Chem. Soc.* 67, 775–781 (2020). oi: 10.1016/j.cdc.2020.100399.
[39] Zayed, E. M. & Mohamed, G. G. Synthesis, spectroscopic, DFT and docking studies, Molecularstructure of new Schiff base metal complexes. *Egypt. J. Chem.* 65, 633–644 (2022). doi: 10.21608/EJCHEM.2021.83871.4116.
[40] Jaafar, F. S. & Alias, M. F. Chemistry of Metalloguanines: An Overview of Their Synthesis Routes and Their Implementations for the Period 2000-2024. *Karbala Int. J. Mod. Sci.* 11, 154–167 (2025). doi: 10.33640/2405-609X.3392.
[41] Morgan, S. M., Diab, M. A. & El-Sonbati, A. Z. Synthesis, molecular geometry, spectroscopic studies and thermal properties of Co(II) complexes. *Appl. Organomet. Chem.* 32, 1–16 (2018). doi: 10.1002/aoc.4305.
[42] Ahmed, Y. J. & Ali, F. M. Biological Activity & Some Transition Elements Complexes For 1, 3, 4 Ox diazole Derivatives On Growth Of Some Pathogenic Bacteria. *Kirkuk J. Sci.* 7, (2012).
[43] Keydel, T. & Link, A. Synthetic Approaches, Properties, and Applications of Acylals in Preparative and Medicinal Chemistry. *Molecules* 29, (2024). doi: 10.3390/molecules29184451.

BIOGRAPHIES OF AUTHORS

Ali Hussein Ali Nima Al-Khazraji is a PhD student at the College of Education for Pure Sciences, Tikrit University, Iraq. He holds a BSc in Chemistry from the University of Baghdad (Ibn Al-Haytham), Iraq, and a MSc from the University of Diyala. His research interests include inorganic chemistry. He has published numerous scientific papers in national and international conferences and journals. He can be contacted via email:: ah244006pep@st.tu.edu.iq

Ahmed A. Irzoqi is a Professor at the College of Education for Pure Science, Tikrit University. He holds a BS in Chemistry from Tikrit University and an MA from the same university. He holds a PhD in Chemistry, specializing in inorganic chemistry. His research interests include phosphine complexes. He has published numerous scientific papers in local and international conferences and journals. To contact him, please email:: ahmedirzoqi@tu.edu.iq.